STEM CELLS

Foxc1 reinforces quiescence in self-renewing hair follicle stem cells

Li Wang,[1] Julie A. Siegenthaler,[2] Robin D. Dowell,[1,3] Rui Yi[1]*

Stem cell quiescence preserves the cell reservoir by minimizing cell division over extended periods of time. Self-renewal of quiescent stem cells (SCs) requires the reentry into the cell cycle. In this study, we show that murine hair follicle SCs induce the *Foxc1* transcription factor when activated. Deleting *Foxc1* in activated, but not quiescent, SCs causes failure of the cells to reestablish quiescence and allows premature activation. Deleting *Foxc1* in the SC niche of gene-targeted mice leads to loss of the old hair without impairing quiescence. In self-renewing SCs, Foxc1 activates Nfatc1 and bone morphogenetic protein (BMP) signaling, two key mechanisms that govern quiescence. These findings reveal a dynamic, cell-intrinsic mechanism used by hair follicle SCs to reinforce quiescence upon self-renewal and suggest a unique ability of SCs to maintain cell identity.

Maintaining a pool of adult stem cells (SCs) is critical for tissue homeostasis and wound repair throughout an organism's life. Self-renewal, a defining property of SCs, is achieved by either symmetrical or asymmetrical cell division, through which new generations of SCs are produced to replenish the SC pool (*1*, *2*). Some SCs can also be kept in a quiescent state for a prolonged period of time to minimize cell turnover (*3*). Although it is well documented that cell extrinsic mechanisms, such as those mediated by the SC niche, play important roles in governing the transition between quiescence and self-renewal, it is unclear whether there are cell-intrinsic mechanisms that respond to self-renewal and promote dividing SCs to return to quiescence. In this study, we investigated largely synchronized murine hair follicle SC (HFSC) populations during early adulthood to probe this layer of SC regulation.

HFSCs reside in an anatomically distinct compartment of the hair follicle, known as the bulge (*4*–*6*). During the adult hair cycle, HFSCs periodically go through the phases of activation and quiescence to maintain the SC population and to produce new hair follicles (*7*). The *Foxc1* transcription factor (TF) has been previously identified as one of the few genes with dynamic histone modification patterns in the HFSCs (*8*), but its expression and function remained unknown. We first monitored *Foxc1* expression during the adult hair cycle using a mouse into which *LacZ* was introduced at the *Foxc1* locus (*Foxc1-LacZ* knock-in mouse) (*9*) and immunofluorescence staining. We did not observe expression of *Foxc1* in the interfollicular epidermis in any of the stages examined (fig. S1). At the first telogen, about postnatal day 18 (~P18), *Foxc1* was absent from the bulge SC compartment but expressed in the infundibulum and sebaceous gland progenitors (Fig. 1A). By anagen III of the HF cycle, *Foxc1* was induced in both the basal and suprabasal bulge layers and the inner root sheath (IRS) (Fig. 1B). In mature HFs, *Foxc1* was strongly expressed in the bulge layers and the IRS (Fig. 1, C to G). When HFs progressed through the catagen and reached the second telogen (~P47), *Foxc1* was again absent in the bulge (Fig. 1, H to J). The

[1]Department of Molecular, Cellular, and Developmental Biology, University of Colorado, Boulder, CO 80309, USA. [2]Department of Pediatrics, Denver-Anschutz Medical Campus, University of Colorado, Aurora, CO 80045, USA. [3]BioFrontiers Institute, University of Colorado, Boulder, CO 80309, USA.
*Corresponding author. E-mail: yir@colorado.edu

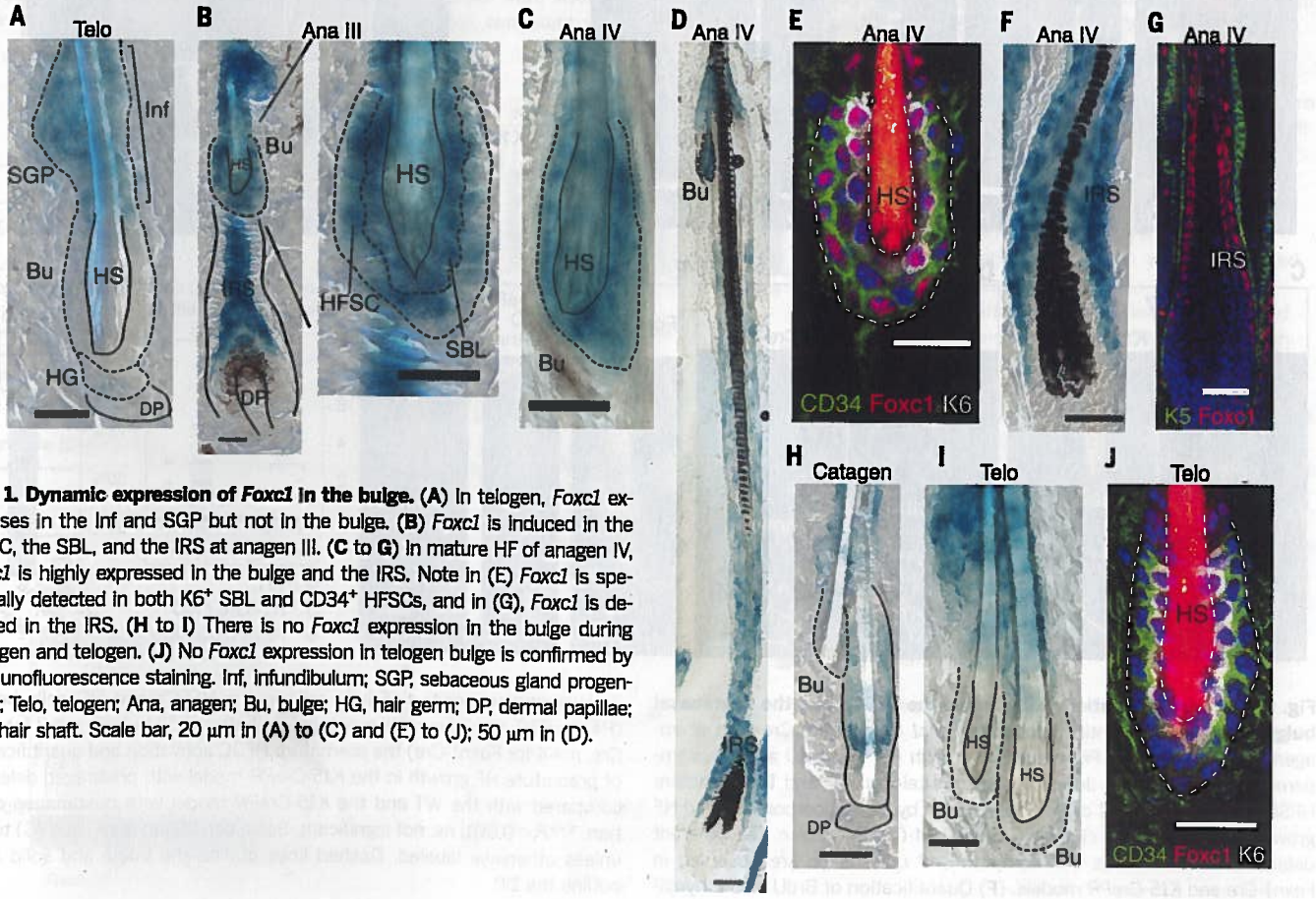

Fig. 1. Dynamic expression of *Foxc1* in the bulge. (**A**) In telogen, *Foxc1* expresses in the Inf and SGP but not in the bulge. (**B**) *Foxc1* is induced in the HFSC, the SBL, and the IRS at anagen III. (**C** to **G**) In mature HF of anagen IV, *Foxc1* is highly expressed in the bulge and the IRS. Note in (E) *Foxc1* is specifically detected in both $K6^+$ SBL and $CD34^+$ HFSCs, and in (G), *Foxc1* is detected in the IRS. (**H** to **I**) There is no *Foxc1* expression in the bulge during catagen and telogen. (**J**) No *Foxc1* expression in telogen bulge is confirmed by immunofluorescence staining. Inf, infundibulum; SGP, sebaceous gland progenitors; Telo, telogen; Ana, anagen; Bu, bulge; HG, hair germ; DP, dermal papillae; HS, hair shaft. Scale bar, 20 μm in (**A**) to (C) and (E) to (J); 50 μm in (D).

induction of *Foxc1* in both those cells positive for keratin 6 (K6$^+$) in the suprabasal bulge layer (SBL), a putative niche for HFSCs (*10*), and the CD34$^+$ HFSCs at the basal bulge layer in anagen but not in telogen was confirmed by immunofluorescence staining (Fig. 1, E and J). Furthermore, by examining old mice in which the hair cycle became asynchronized and all different hair cycle stages were observed in a single animal, we validated that the expression of *Foxc1* inherently correlates with the hair cycle (fig. S1).

We then investigated *Foxc1* function by conditionally deleting *Foxc1* [conditional knock out (cKO)] in the skin of mice. *K14-Cre* deletes *Foxc1* in all skin lineages. *Foxn1-Cre* deletes *Foxc1* in the SBL but not in the HFSCs. *K15-CrePR* deletes *Foxc1* in the HFSCs but not in the SBL upon induction (Fig. 2A and fig. S2). All wild-type (WT) and cKO animals were born at the expected Mendelian ratios (fig. S3A) and developed normal skin neonatally, consistent with the lack of *Foxc1* expression in embryonic skin progenitors (fig. S3, B and C).

Compared with the WT HFs, which usually entered anagen at ~P70 to P75, the *K14-Cre* cKO HFs had a much shortened telogen: The HFs entered anagen prematurely by the middle of the second telogen at ~P64 (as revealed by the darkened skin) and grew hair coat by P70 (Fig. 2B). We then examined HFSC activation in WT and cKO animals during the second adult telogen. At P47, we observed no signs of HF growth or HFSC division. However, loss of the old hair follicle (also known as club hair) was evident (Fig. 2C). By P60, HF growth was initiated in cKO mice, as indicated by widespread bromodeoxyuridine (BrdU) incorporation into both the HFSCs and hair germs (HGs, the progenitors that fuel hair growth) (Fig. 2, D and F). By P64, whereas cKO animals produced mature HFs, WT animals were still in quiescent telogen (fig. S4A). In the *Foxn1-Cre* cKO mice, in which *Foxc1* was deleted in the SBL but not in the HFSCs, no premature HF growth was observed, although the loss of club hair was evident (Fig. 2E, left). In contrast, in the *K15-CrePR* model in which *Foxc1* was deleted before anagen, premature HF growth was observed without the loss of club hair at P60 (Fig. 2E, middle, and 2F). In the *K15-CrePR* model, in which *Foxc1* was deleted after anagen, neither premature HF growth nor the loss of club hair was observed at P60 (Fig. 2E, right, and 2F). By dyeing hair at P21 and observing subsequent loss of the dyed hair, we found that the club hair was lost late in the second anagen (~P33 to P35) in the *K14-Cre* and *Foxn1-Cre* cKO mice (fig. S4, B and C). Morphological examination showed that the loss of club hair was correlated with upward movement of the club hair, likely caused by reduced cell adhesion but not by abnormal apoptosis or proliferation of the SBL (fig. S4, D to F).

The widespread loss of club hair was further confirmed by flow cytometry analysis, by which HFSCs were detected as *H2BGFP^{hi}/CD34^{hi}/α6^{hi}* and *H2BGFP^{hi}/CD34^{hi}/α6^{lo}* populations in WT skin (*5*). The *H2BGFP^{hi}/CD34^{hi}/α6^{lo}* population marks a cell population sandwiched between the club hair and the new hair follicle, characteristic of the two-bulge formation in WT skin (*5*) (fig. S5A). Consistent with the morphological results, we observed a progressive loss of the *H2BGFP^{hi}/CD34^{hi}/α6^{lo}* population in the *K14-Cre* and *Foxn1-Cre* cKO between P30 and P47 (fig. S5, B and C). CD34 expression levels in the KO HFSCs were also

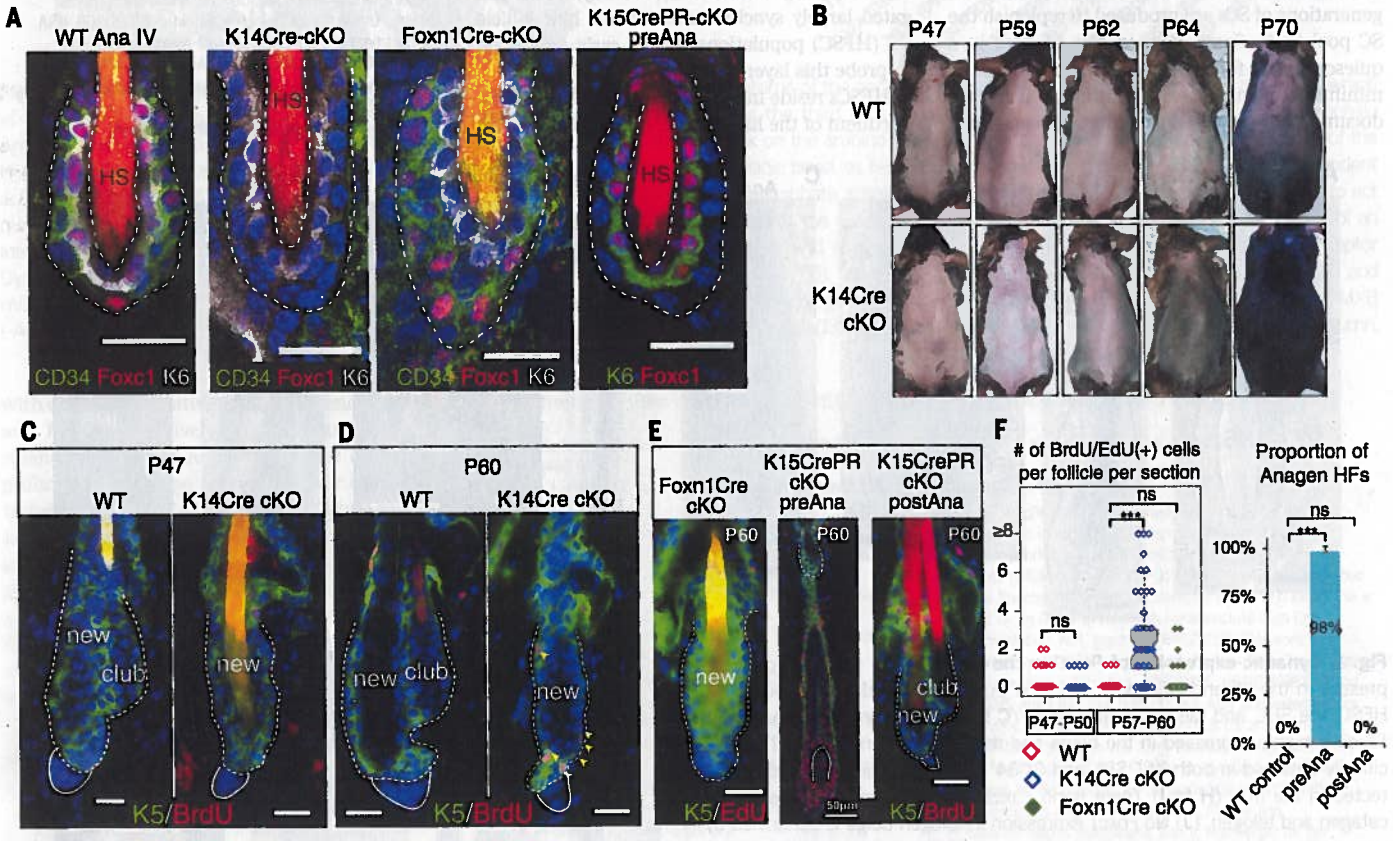

Fig. 2. *Foxc1* is differentially required by the HFSCs and the suprabasal bulge layer. (**A**) Differential deletion of *Foxc1* by different Cre lines at anagen (P26 to P30). (**B**) Premature HF growth of *Foxc1* cKO animals, compared with WT animals, during the second telogen. (**C** and **D**) Premature HFSC activation in *Foxc1* cKO mice is shown by BrdU incorporation and HF growth and the loss of club hair in the *K14-Cre* cKO mice. (**E**) Different defects in club hair loss and compromised quiescence are observed in *Foxn1-Cre* and *K15-CrePR* models. (**F**) Quantification of BrdU or 5-ethynyl-2′-deoxyuridine–positive (EdU$^+$) cells in the HFSCs and HG cells before (P47 to P50, $n = 3$ for each genotype) and after (P57 to P60, $n = 3$ for *K14-Cre*, $n = 4$ for *Foxn1-Cre*) the premature HFSC activation and quantification of premature HF growth in the *K15-CrePR* model with preanagen deletion, compared with the WT and the *K15-CrePR* model with postanagen deletion. ***$P < 0.001$; ns, not significant. Scale bar, 20 μm in (A) and (C) to (E) unless otherwise labeled. Dashed lines outline the bulge and solid lines outline the DP.

reduced (fig. S5D). These data indicate that *Foxc1* is required to restrict HFSCs from premature activation and to maintain the club hair. The *Foxn1-Cre* cKO results suggest that *Foxc1* is required by the SBL to maintain the club hair. The *K15-CrePR* cKO results reveal an intrinsic requirement of *Foxc1* by HFSCs and suggest that temporal induction of *Foxc1* in the activated HFSCs during anagen is required to reinforce quiescence.

To determine the effect of loss of *Foxc1* on HFSC quiescence, we performed RNA sequencing (RNA-Seq) at P47 when both WT and *K14-Cre* cKO HFSCs were in telogen. Genes associated with quiescence of HFSCs, including *Bmp6* (*11*) and *Fgf18* (*12*, *13*), and HFSC markers (*4*, *5*, *14*), including *CD34*, were among the substantially down-regulated genes, whereas genes associated with HFSC activation were up-regulated in the cKO mice (Fig. 3A). Signature genes characteristic of quiescent SCs (*3*) were dysregulated (Fig. 3A). Global analysis revealed that genes involved in cell division were markedly up-regulated (fig. S6A). We then confirmed by quantitative polymerase chain reaction (qPCR) the down-regulation of *Bmp6*, *CD34*, and *Fgf18* and the up-regulation of cell cycle genes in the HFSCs purified from each model. Consistent with the cell-intrinsic requirement of *Foxc1* in the HFSCs during anagen, changes of gene expression were only observed in the *K14-Cre* and *K15-CrePR* models, in which *Foxc1* was constitutively deleted or specifically deleted in the HFSCs before anagen, respectively. Also, changes of gene expression were not seen in the *Foxn1-Cre* and *K15-CrePR* models, in which *Foxc1* was deleted in the SBL but not in the HFSCs, or specifically deleted in the HFSC after anagen, respectively (Fig. 3B and fig. S7).

Next, we performed gene set enrichment analysis (GSEA) using published HFSC and progenitor data sets (*15*). Quiescent *Foxc1* KO HFSCs (P47) were more similar to HG progenitors that are poised for activation than to quiescent HFSCs (Fig. 3C and fig. S8). We also observed a strong similarity between *Foxc1* and *Lhx2* cKO HFSCs in their molecular signature (fig. S8). We then performed principal component analysis using data sets from the quiescent or activated HFSCs (*8*, *12*, *16*), the HGs (*12*), the transit-amplifying cells (TACs) (*8*), and our RNA-Seq data. We found that activated HFSCs (P28) and dividing HFSCs destined for differentiation (P20) (*16*) were intermediate populations between quiescent HFSCs and HG progenitors. The P47 *Foxc1* KO HFSCs were grouped most closely with activated HFSCs and clearly distinct from quiescent HFSCs (Fig. 3D). These data provide a global view for the sensitized cellular state of the *Foxc1* KO HFSCs before the premature SC activation.

To determine the mechanism of Foxc1's action, we analyzed differentially expressed (DE) genes in *Foxc1* WT and KO HFSCs between P29 and P31, when the HFSCs are activated and when *Foxc1* is highly expressed. Genes associated with HFSC quiescence, HFSC markers, and adhesion were notably down-regulated, and cell cycle regulators were strongly up-regulated in the cKO mice, consistent with the observed phenotypes (Fig. 4A and fig. S6B). These data suggest that the transient expression of *Foxc1* maintains SC adhesion and promotes the transition back to quiescence when the HFSCs undergo self-renewal.

Next, we mapped open chromatin regions and TF occupancy in the WT and KO HFSCs using an assay for transposase-accessible chromatin using sequencing (ATAC-Seq) (*17*). We analyzed published chromatin immunoprecipitation sequencing (ChIP-Seq) data for Sox9 (*18*), Tcf3/4 (*19*), and Lhx2 (*20*) in HFSCs and observed strong overlaps between ChIP-Seq and ATAC-Seq peaks, which validated the detection of TF occupancy by ATAC-seq (fig. S9, A to C). To determine Foxc1 recognition motifs, we analyzed a Foxc1 ChIP-Seq data set (*21*). De novo motif discovery retrieved Foxc1-binding sites that were best matched by previously determined Foxa2 and Foxa1 recognition motifs (fig. S9D). Notably, Foxa2 and Foxc1 were validated to bind to the same enhancer sequences (*22*), consistent with our findings. Both *Foxa1* and *Foxa2* loci are epigenetically silenced in HFSCs (fig. S10), which suggests that Foxc1 is responsible for these binding sites. We then intersected our ATAC-seq peaks harboring the Foxc1 recognition motifs with DE genes ($P < 0.01$) in the *Foxc1* KO HFSCs. We identified 104 genes likely to be targeted by Foxc1 (table S1). Among these putative targets, 85 (81.7%) were down-regulated in the *Foxc1* KO HFSCs (fig. S9E). Several genes involved in regulating HFSC quiescence were found to contain Foxc1-binding sites in their promoter or enhancer regions, including *Bmp2* (*23*), *Foxp1* (*24*), *Nfatc1* (*25*, *26*), and *Prlr* (*26*, *27*).

A

P47 HFSC RNA-seq cKO vs WT

HFSC marker	CD34 (-2.3x), S100a4 (-2.2x)
Negative regulator of HFSC activation	Fgf18 (-2.5x), Bmp6 (-3.3x), Grem1 (-2.0x)
Positive regulator of HFSC activation	Ptch2 (+8.4x), Gli1 (+2.2x)
Quiescent SC signature (Enriched)	Zyx (-2.5x), Smarca2 (-1.9x)
Quiescent SC signature (Depleted)	Top2a (+4.7x), Ccnb1 (+3.8x), Ccna2 (+3.0x), Anln (+3.9x), Sgol1 (+3.9x)

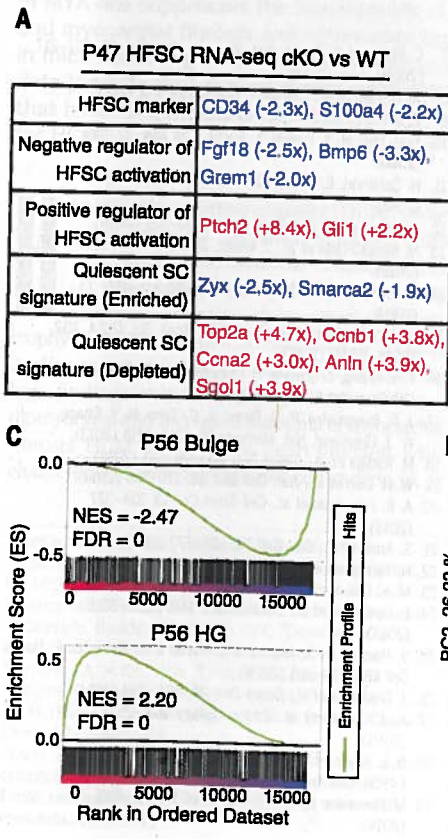

Fig. 3. *Foxc1* KO HFSCs fail to return to quiescence. (**A**) Functional classification of selected DE gene in P47 KO HFSCs. Red and blue mark up- and down-regulated genes in the KO HFSCs, respectively. (**B**) qPCR validation of down- and up-regulated genes in the HFSCs isolated from different cKO models at the second telogen (P47 to P60, $n \geq 3$ for each genotype, $^*P < 0.05$). (**C**) GSEA comparison of P47 KO transcriptome to telogen bulge and HG signature genes. NES, normalized enrichment score; FDR, false discovery rate. (**D**) Principal component analysis of P47 *Foxc1* KO transcriptome and profiling data from WT HFSCs, HGs, and TACs. Linear discriminant analysis groups *Foxc1* KO transcriptome to activated HFSCs.

A

P30 HFSC RNA-seq cKO vs WT

HFSC marker	Cd34 (-2.0x), Krt15 (-3.6x), Lgr6 (-4.4x), S100a4 (-6.0x)
Signaling	Bmp2 (-4.5x), Bmp6 (-2.6x), Fgf18 (-8.7x), Prlr (-2.2x)
Cell adhesion	Cadm1 (-3.9x), Cadm4(-4.0x), Cldn4(-2.4x), Dsg3(-1.8x), Tgm5 (-28.2x)
Cell cycle	Ccnb2 (+2.4x), Cdk1 (+2.4x), Cenpe (+2.5x), Cdc20 (+1.9x), Mki67 (+2.1x), Top2a (+1.9x)

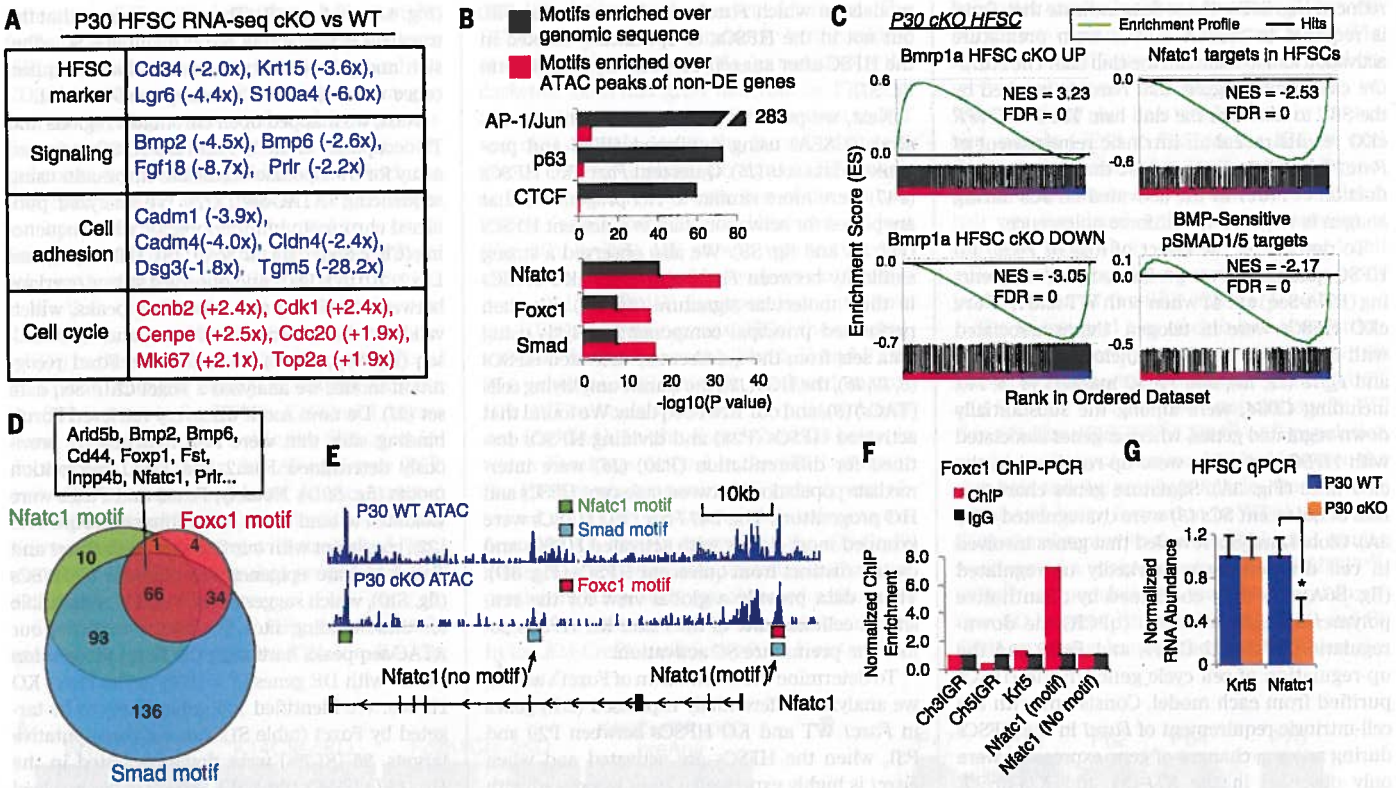

Fig. 4. *Foxc1* activates quiescence gene networks. **(A)** Functional classification of selected DE gene in P30 KO HFSCs. **(B)** Comparison of enriched TF motifs against genomic sequences and against the peaks covering the non-DE genes in P30 KO HFSCs. **(C)** GSEA of bone morphogenic proteins (BMP)–responsive genes and Nfatc1 targets in P30 KO HFSCs. **(D)** Venn diagram of the DE genes in P30 KO HFSCs that contain motifs of Foxc1, Smad, and Nfatc1 shows a coregulated gene network. **(E)** ATAC-seq track of the *Nfatc1* locus. Location of Nfatc1, Smad, and Foxc1 motifs are shown in the peak region. **(F)** ChIP-PCR analysis of Foxc1 confirms association of Foxc1 to the predicted binding site in the *Nfatc1* locus. **(G)** DE of Foxc1 targets, *Krt5* and *Nfatc1*, in the WT and KO HFSCs (*$P < 0.05$).

We further dissected pathways that are downstream from *Foxc1*. Because ATAC-seq provided a comprehensive survey for all TF-binding sites in the genome, we analyzed the top TF hits in our ATAC-seq. Overall in the HFSCs, motifs representing AP-1/c-Jun, p63, and CTCF were the most enriched sequences that were detected by ATAC-seq, consistent with high expression levels and the widespread roles of these TFs in the skin (Fig. 4B). However, when we specifically searched the subset of ATAC-seq peaks that cover the DE genes identified in the *Foxc1* KO HFSCs against ATAC peaks of non-DE genes, motifs representing Foxc1, Nfatc1, and Smad, which reflect the BMP signaling pathway, were significantly enriched (Fig. 4B). Furthermore, GSEA comparison showed that direct targets of Nfatc1 (*28*) and pSMAD1/5 (*29*) were considerably enriched and largely down-regulated in the *Foxc1* KO HFSCs, which positively linked the *Foxc1* KO HFSCs to the compromised BMP signaling pathway and loss of *Nfatc1* in the HFSCs (*29*, *30*) (Fig. 4C). Sixty-six of these genes—including *Bmp2*, *Bmp6*, *Foxp1*, *Inpp4b*, *Nfatc1*, and *Prlr*—were likely coregulated by Foxc1, Nfatc1, and Smad (Fig. 4D and tables S2 and S3). Such a combinatorial action of these TFs is illustrated by the *Nfatc1* locus (Fig. 4E). The direct regulation of *Nfatc1*, *Bmp6*, and *Hspb8* by Foxc1 was confirmed by ChIP-PCR and qPCR (Fig. 4, F and G, and fig. S11). Because *Hspb8* was confirmed as a Smad target (*29*), it is an example coregulated by Foxc1 and Smad. Overall, 343 out of 421 DE genes are likely controlled by *Foxc1* directly (104) or by *Nfatc1* (170) and *Smad* (328) indirectly, which indicates a collaborative gene regulatory network between *Foxc1* and *Nfatc1*, as well as BMP signaling, two critical regulatory networks governing the quiescence of HFSCs (*11*, *12*, *23*, *25*, *30*, *31*).

In conclusion, we have uncovered a dynamic and cell-intrinsic mechanism mediated by *Foxc1* that is induced to promote quiescent SC identity in response to SC activation. Our findings also suggest that quiescent SCs actively sense the change of their cellular states and use transient gene expression to reinforce their identity. Investigation of such adaptive mechanisms should provide new insights into SC maintenance during tissue homeostasis and injury repair.

REFERENCES AND NOTES

1. K. W. Orford, D. T. Scadden, *Nat. Rev. Genet.* **9**, 115–128 (2008).
2. S. He, D. Nakada, S. J. Morrison, *Annu. Rev. Cell Dev. Biol.* **25**, 377–406 (2009).
3. T. H. Cheung, T. A. Rando, *Nat. Rev. Mol. Cell Biol.* **14**, 329–340 (2013).
4. T. Tumbar *et al.*, *Science* **303**, 359–363 (2004).
5. C. Blanpain, W. E. Lowry, A. Geoghegan, L. Polak, E. Fuchs, *Cell* **118**, 635–648 (2004).
6. G. Cotsarelis, T. T. Sun, R. M. Lavker, *Cell* **61**, 1329–1337 (1990).
7. C. Blanpain, E. Fuchs, *Nat. Rev. Mol. Cell Biol.* **10**, 207–217 (2009).
8. W.-H. Lien *et al.*, *Cell Stem Cell* **9**, 219–232 (2011).
9. T. Kume *et al.*, *Cell* **93**, 985–996 (1998).
10. Y. C. Hsu, H. A. Pasolli, E. Fuchs, *Cell* **144**, 92–105 (2011).
11. N. Oshimori, E. Fuchs, *Cell Stem Cell* **10**, 63–75 (2012).
12. V. Greco *et al.*, *Cell Stem Cell* **4**, 155–169 (2009).
13. M. Kimura-Ueki *et al.*, *J. Invest. Dermatol.* **132**, 1338–1345 (2012).
14. R. J. Morris *et al.*, *Nat. Biotechnol.* **22**, 411–417 (2004).
15. A. Subramanian *et al.*, *Proc. Natl. Acad. Sci. U.S.A.* **102**, 15545–15550 (2005).
16. Y. V. Zhang, J. Cheong, N. Ciapurin, D. J. McDermitt, T. Tumbar, *Cell Stem Cell* **5**, 267–278 (2009).
17. J. D. Buenrostro, P. G. Giresi, L. C. Zaba, H. Y. Chang, W. J. Greenleaf, *Nat. Methods* **10**, 1213–1218 (2013).
18. M. Kadaja *et al.*, *Genes Dev.* **28**, 328–341 (2014).
19. W.-H. Lien *et al.*, *Nat. Cell Biol.* **16**, 179–190 (2014).
20. A. R. Folgueras *et al.*, *Cell Stem Cell* **13**, 314–327 (2013).
21. S. Amin *et al.*, *Dev. Cell* **32**, 265–277 (2015).
22. H. Yamagishi *et al.*, *Genes Dev.* **17**, 269–281 (2003).
23. M. V. Plikus *et al.*, *Nature* **451**, 340–344 (2008).
24. E. Leishman *et al.*, *Development* **140**, 3809–3818 (2013).
25. V. Horsley, A. O. Aliprantis, L. Polak, L. H. Glimcher, E. Fuchs, *Cell* **132**, 299–310 (2008).
26. J. Goldstein *et al.*, *Genes Dev.* **28**, 983–994 (2014).
27. A. J. Craven *et al.*, *Endocrinology* **142**, 2533–2539 (2001).
28. B. E. Keyes *et al.*, *Proc. Natl. Acad. Sci. U.S.A.* **110**, E4950–E4959 (2013).
29. M. Genander *et al.*, *Cell Stem Cell* **15**, 619–633 (2014).